

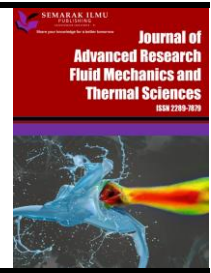


Journal of Advanced Research in Fluid Mechanics and Thermal Sciences

Journal homepage:

https://semarakilmu.com.my/journals/index.php/fluid_mechanics_thermal_sciences/index

ISSN: 2289-7879



Parametric Study of Photovoltaic System Integrated with Organic Phase Change Material using ANSYS

Mohd Afzanizam Mohd Rosli^{1,2*}, Nurfarhana Salimen¹, Nurul Izzati Akmal Muhamed Rafaizul¹, Suhaimi Misha¹, Norli Abdullah³, Safarudin Ghazali Herawan⁴, Avita Ayu Permanasari⁵, Faridah Hussain⁶

¹ Faculty of Mechanical Engineering, Universiti Teknikal Malaysia Melaka, Hang Tuah Jaya, 76100 Durian Tunggal, Melaka, Malaysia

² Centre for Advanced Research on Energy, Universiti Teknikal Malaysia Melaka, Hang Tuah Jaya, 76100 Durian Tunggal, Melaka, Malaysia

³ Chemistry Department, Centre for Defence Foundation Studies, 57000 Kuala Lumpur, National Defence University of Malaysia, Malaysia

⁴ Industrial Engineering Department, Faculty of Engineering, Bina Nusantara University, Jakarta, 11430, Indonesia

⁵ Department of Mechanical Engineering, Faculty of Engineering, State University of Malang, Jl. Semarang No.5, Malang 65145, East Java, Indonesia

⁶ SIRIM Standards Technology Sdn. Bhd., Seksyen 15, 40200 Shah Alam, Selangor, Malaysia

ARTICLE INFO

ABSTRACT

Article history:

Received 21 January 2023

Received in revised form 20 April 2023

Accepted 27 April 2023

Available online 17 May 2023

Keywords:

Crude palm oil; Phase Change Material; PV-PCM; Photovoltaic; simulation

Thermal management is essential in photovoltaic (PV) systems for enhancing PV performance. Passive cooling with a phase transition material (PCM) is one method for managing overheated PV. Crude palm oil (CPO) is preferred in Malaysia since it is both sustainable and inexpensive. To assess the feasibility of CPO as a PCM, a parametric analysis focusing on the PV-PCM tilt angles, PCM thickness, and PCM encapsulation material was carried out numerically. ANSYS computational fluid dynamics software is used in this work. The two-dimensional model is used to simulate a monocrystalline PV surface with macro-encapsulated PCM placed among two aluminium layers. Each parametric analysis's temperature distribution on PV surfaces and temperature contour for PV-PCM for tilting angle and PCM thickness are also discussed. Validation work was also performed with 9.73% errors that were within the allowed range. The result reveals that when the tilt angle is near-vertical (90°) the natural convection flows more rapidly. The system's average front surface appears to achieve the melting point completely faster. The optimum thickness for CPO to perform is 80mm, which can store heat for around 4000s (66.67mins). Aluminium outperforms stainless steel and copper as a PCM encapsulant since it facilitated the melting process by absorbing more heat. CPO with 80mm thickness, aluminium encapsulated, and vertical orientation has significant potential for thermoregulation in systems, especially in Malaysian weather (27°C).

* Corresponding author.

E-mail address: afzanizam@utem.edu.my

<https://doi.org/10.37934/arfmts.106.1.7689>

1. Introduction

Ever since the depletion of nonrenewable energy resources like oil per barrel, liquid petroleum gas (LPG), and charcoal, with greater demand and supply throughout the decades, the research on the perspective of accessible renewable sources seems to have become significant [1]. Solar energy as a source of electric power and fluid heating provides numerous environmental, economic, and even maintenance benefits. With these advantages, investment in this sort of energy tends to increase as a result of global concern for the environment and climate change [2]. Photovoltaic (PV) systems have been increasingly popular in generating thermal and electrical energy as a green alternative to energy supply in recent years. Because photovoltaic systems get heat and light energy directly from the sun, they can overheat over time. The photovoltaic effect of a solar panel is facilitated by photons with energy higher than the band gap energy, while the rest of the photon energy is transformed into heat, leading the solar cell temperature to rise and therefore diminishing the panel's electrical performance. This temperature increase has a negative impact on the open-circuit voltage (V_{oc}), fill factor, and output power [3]. Overheating is a big issue with PV systems, affecting efficiency and performance as well as potentially destroying the system in the long run. Thus, numerous cooling approaches, such as active and passive cooling methods, have been devised.

Cooling systems based on phase change materials (PCM) have recently gained popularity for lowering PV module temperatures and increasing efficiency [4]. The main advantage of passive cooling technologies, such as phase change materials, is their self-sufficiency and low extra power consumption while maintaining a basic model [5]. PCM could gather or release a specific amount of external sensible heat during its phase transition for beneficial heat or cooling without affecting the material's internal temperature. Depending on the properties of the chosen material, this process can store a large amount of heat or cold [6]. Thermal energy is stored as latent heat, which is subsequently used to weaken or establish chemical bonds while the body's kinetic energy is preserved. As a result, they may be used to manage the temperature of photovoltaic (PV) and concentrated photovoltaic (CPV) systems [7].

A list of criteria is needed to choose PCM that suits certain applications and climate effects. According to Aridi and Yehya [8], there are a few properties to look into when choosing the PCM including its thermal, physical, chemical, kinetic, economic, and environmental. One of the first properties to consider is thermal, and it must have good heat transfer, high latent heat energy, and a suitable phase transition temperature concerning its climate condition. It must have a high density and specific heat capacity, a small volume change, a low vapour pressure, and a favourable phase equilibrium for physical properties. Meanwhile, it should be chemically compatible with other materials, have long-term stability, and be non-toxic, non-corrosive, and non-flammable. There must be no sub-cooling and a sufficient crystallization rate for kinetic properties. PCMs that are economically feasible are those that are simple, plentiful, and widely available. It must be recyclable, have a low negative effect on the environment, and be non-polluting throughout its entire service.

The two major categories of PCMs are organic and inorganic. These are further subdivided into paraffin, non-paraffin (including fatty acids), salt hydrates, and metallic PCMs [9]. Organic PCM is made up of both paraffin and non-paraffin components. Non-paraffin is derived from renewable sources such as plants and animals, whereas paraffin is derived from non-renewable sources such as petroleum. Non-paraffin organic compounds have the broadest range of materials and properties, although paraffin is the most commonly utilized commercially [9].

Crude Palm Oil (CPO) is a significant fatty acid supply in Malaysia, and it is suitable for use when temperatures vary between 20°C and 30°C. More than 80% of the world's considerable palm oil output is accounted for by Indonesia, Malaysia, and Thailand. Large firms that generate crude palm

oil dominate several countries. This contributes to economic growth for residents and state governments across the country [10]. Also, T. Sarikarin *et al.*, [11] state that palm wax is utilized instead of paraffin wax because it has a greater melting point and lowers the cost of PCMs.

Several scholars have worked on the development of PV-PCM systems. Many factors can increase the value of the PV's temperature reduction. J. Zhao *et al.*, [12] used a comparison of traditional PV and PV-PCM to demonstrate the effectiveness of the PV-PCM system. By adding PCM to PV, the temperature was reduced by 24.9°C, indicating that PCM has substantial potential in regulating PV temperature. Following some evidence of the PV-PCM system's effectiveness, various research has focused on adjusting the parametric elements such as PV-PCM tilting angle [13-16], PCM thickness [17-19], and more. Numerical and experimental work was done by A. Abdulmunem *et al.*, [15] who studied the effect of various PV-PCM tilting angles from 0°, 30°, 60°, to 90° towards the backside of the heat sink. The results were the PCM melting process decreases as the tilting angle increases due to the natural convection heat flows within the PCM. According to S. Bantová *et al.*, [20], the material for PCM encapsulation, particularly metal type, has also been explored to further improve the system. They tested the compatibility of four different metals with PCMs such as aluminium, brass, copper, and carbon steel. Aluminium was found to be the best alternative for PCM containers. However, to further extend the capability of cooling the PV, some researchers innovate the system into a hybrid PVT-PCM system [21,22].

Based on previous studies on lowering the PV-PCM temperature, the study focuses on selecting the best parameter in optimising the system using crude palm oil as the PCM is still insufficient. Several studies have been conducted to determine the best thickness for CPO, palm oil, or even palm wax as PCM, but research into the best container material specifically for CPO as PCM and its tilting angle is still insufficient to conclude the optimisation of the system with CPO as its PCM. Hence, the key objectives of this work are to evaluate the temperature differences, distribution, and contour of the PV-PCM via a parametric study that includes PV-PCM tilt angles, PCM thickness, and PCM encapsulation material, all of which were performed numerically using ANSYS 2022 R1. Also, the temperature distribution for the PV-PCM will be compared with the system without PCM to highlight the significance of the work. Validation work is also included in this paper. At the end of the analysis, the optimal tilt angle, PCM thickness, and encapsulation material will be determined.

2. Methodology

2.1 Model Geometry

ANSYS Design Modeler was used to create the 2-D model geometry illustrated in Figure 1. The PV-PCM system has a height of 132mm. In this approach, the exterior photovoltaic (PV) surface, aluminium, and phase change material (PCM) components are macro-encapsulated and put beneath the PV cell. Layers are represented by the model parameters, with aluminium and PCM having thicknesses of 4mm and 20mm, respectively. The model's external PV surface is on the left side.

For the PV-PCM various tilt angles orientation, the system is inclined from 0°(horizontal), 30°,60°, to 90°(vertical). Then, the thickness of the PCM is varied from 20mm to 100mm with an inclination of 20mm. For the last section, the geometry of the PV-PCM stays the same as the origin as shown in Figure 1.

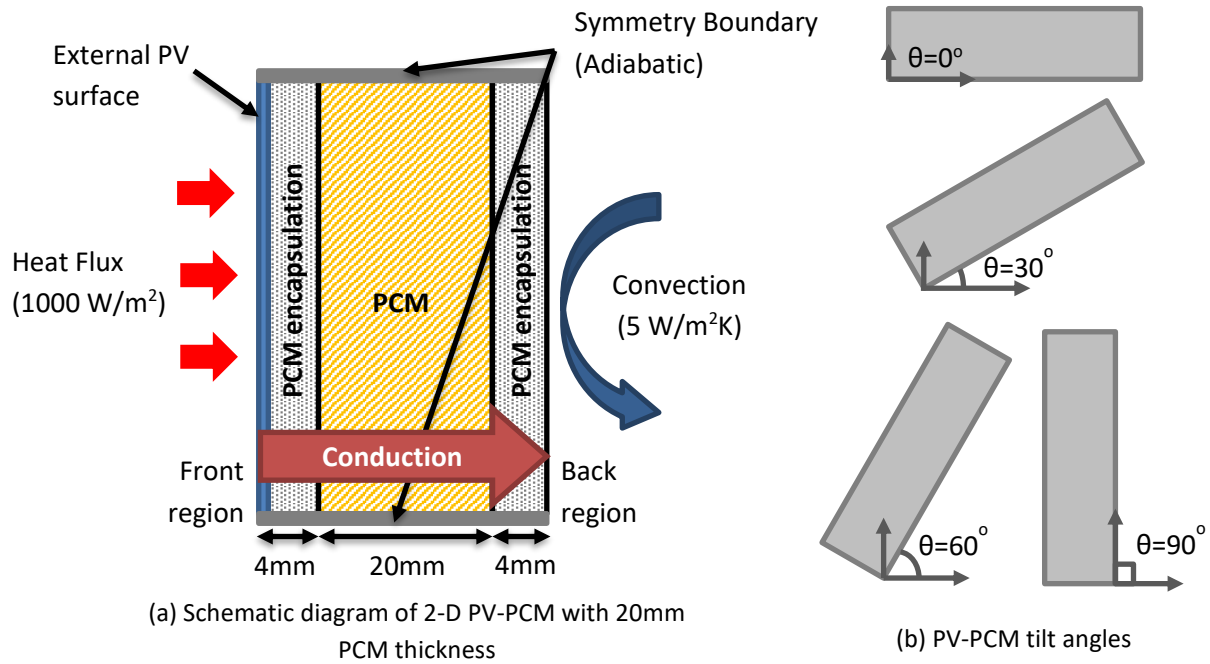


Fig. 1. Model geometry design for the current work, (a) Schematic diagram of 2-D PV-PCM, and (b) PV-PCM tilt angles

2.2 Mesh Independence Study

As the completed mesh, a 2mm element size mesh was selected. Meshes of element sizes of 3mm, 4mm, and 5mm yield rising temperatures of 0.03K, 0.05K, and 0.26K, respectively, although finer meshes with element sizes of 0.5mm and 1mm have no impact as shown in Table 1. The mesh metrics skewness describes the quality of the produced mesh. It is in a good range for this value [23]. The total number of nodes and elements created is 1139 and 924, respectively.

Table 1
 Mesh Independence Study

Element size (mm)	Coarsest ➔ Finest						
	5	4	3	2	1.5	1	0.5
Number of elements	162	231	484	924	1672	3696	14784
Number of nodes	252	340	630	1139	1958	4123	15635
Average Skewness	$4.7e^{-4}$	$1.3e^{-10}$	$4.4e^{-4}$	$7.1e^{-5}$	$9.0e^{-4}$	$1.3e^{-10}$	$2.7e^{-5}$
Temperature front PV-PCM system at t=100s (K) (y=0.01m, x=0.014m)	293.44	293.23	293.21	293.18	293.20	293.18	293.18

2.3 Governing Equations

ANSYS Fluent was used to solve the two-dimensional model, and several partial differential equations, including the continuity equation (mass conservation), Navier-Stokes equation (momentum), and energy equation. Since there are two types of regions that needed to be solved, which are solid component region and phase change material region. For the solid domain,

conduction is the only heat transfer mechanism involved which makes the energy equation used for these regions as follows [24]

$$\rho c_{p,solid} \left(\frac{\partial T_{solid}}{\partial t + \vec{v} \cdot \nabla T} \right) = \nabla \cdot (k_{solid} \nabla T_{solid}) \quad (1)$$

where ρ represents density, $c_{p,solid}$ is the specific heat capacity of the solid component, and k_{solid} is the thermal conductivity of the solid material.

As for the phase change material domain, the mass, momentum, and energy are determined by slightly different equations as follows

Continuity equation (mass conservation) [15],

$$\frac{\partial \rho}{\partial t} + \frac{\partial(\rho u)}{\partial x} + \frac{\partial(\rho v)}{\partial y} = 0 \quad (2)$$

where ρ represents density, u , and v are fluid velocity components in the x and y directions, respectively, and t is the time for the unsteady-state case.

Navier-Stokes equation (momentum) [15],

a) u-momentum equation (x-direction)

$$\frac{\partial}{\partial t}(\rho u) + \frac{\partial}{\partial x}(\rho u u) + \frac{\partial}{\partial y}(\rho u v) = -\frac{\partial \rho}{\partial x} + \frac{\partial}{\partial x} \left(\mu \frac{\partial u}{\partial x} \right) + \frac{\partial}{\partial y} \left(\mu \frac{\partial u}{\partial y} \right) + S_u \quad (3)$$

b) v-momentum equation (y-direction)

$$\frac{\partial}{\partial t}(\rho v) + \frac{\partial}{\partial x}(\rho u v) + \frac{\partial}{\partial y}(\rho v v) = -\frac{\partial \rho}{\partial y} + \frac{\partial}{\partial x} \left(\mu \frac{\partial v}{\partial x} \right) + \frac{\partial}{\partial y} \left(\mu \frac{\partial v}{\partial y} \right) + S_v \quad (4)$$

S_u and S_v is the enthalpy balance equation in the x and y directions for calculating the liquid fraction of the PCM since to simulate the melting process in the PCM, the enthalpy porosity technique is used. The enthalpy balance equation, S is shown as follows [24]

$$S = \frac{(1-\beta)^2}{(\beta^3 + \emptyset)} A_{mush} (\vec{V} - \vec{V}_p) \quad (5)$$

where β represents liquid volume fraction, A_{mush} is the mushy zone constant which is set to 10^5 , \emptyset is a small number to avoid division by zero and it is equal to 0.001, and \vec{V}_p is the solid velocity.

Furthermore, the energy equation specifically for PCM denotes as follows

$$\frac{\partial}{\partial t}(\rho H) + \nabla \cdot (\rho \vec{V} H) = \nabla \cdot (k \nabla T) + S \quad (6)$$

where H is the enthalpy of material, ρ is the density, \vec{V} is the fluid velocity, S is the source term.

For modelling the buoyancy effects for natural convection within the PCM, the Boussinesq model is used as follows

$$(\rho - \rho_0) \approx -\rho_0 \beta (T - T_0) g \quad (7)$$

where ρ_0 is the constant density of the flow, T_0 is the operating temperature, β represents the thermal expansion coefficient, and g is the gravitational force value. This approximation is only valid when $\beta(T - T_0) \ll 1$.

2.4 Boundary Conditions

As illustrated in Figure 1, the front of the PV-PCM, also referred to as the external PV surface, gets a direct heat flux of 1000 W/m^2 , whilst the back of the PV-PCM obtains convective heat transfer (h) at $5 \text{ W/m}^2\text{K}$, with an average surrounding temperature of 27°C [25]. The edges of the system are aligned with the symmetry boundary. Aluminium and PCM contact areas and interfaces are connected.

2.5 Numerical Approach and Assumptions

Several assumptions were made before beginning the numerical approach method. The following assumptions were used for the overall model simulation.

- i. Melting is a two-dimensional transient process [26].
- ii. PCM does not generate thermal energy [26].
- iii. The PCM involves mainly heat conduction as well as no liquid flow in the PCM body [27].
- iv. During the process, the thermal properties of the PCM stay constant, and the Boussinesq model is utilized to determine the buoyancy force term [28].
- v. Heat resistance is reduced between the PCM material to the PV panel, as well as between the PCM material and the aluminium frame [27].

The numerical approach was implemented using ANSYS Fluent, which used the finite element method to solve the partial differential equations necessary to describe the two-dimensional PV-PCM system with double precision code. The general settings were set to transient mode to ensure that the results returned are time-dependent, which is what must be fully focused on. The thermophysical properties of aluminium, copper, CPO, stainless steel, and PV cells are shown in Table 2.

Table 2
 Thermophysical properties of materials

Material	PCM encapsulation			PCM	PV Surface
	Aluminium [29]	Copper [30]	Stainless Steel	Crude Palm Oil	PV Cell [31]
Thickness (mm)	4	4	4	20, 40, 60, 80, 100	-
Thermal Conductivity ($\text{W/m}\cdot\text{K}$)	211	398	-	0.17 [32]	148
Density (kg/m^3)	2675	8900	8000 [33]	895 [34]	2330
Specific heat capacity ($\text{J/kg}\cdot\text{K}$)	903	386	502.42	2080 [34]	677
Latent heat capacity (J/kg)	-	211 500	16.2 [33]	23840 [35]	-
Viscosity (kg/ms)	-	-	-	0.0345 [32]	-
Melting temperature ($^\circ\text{C}$)	-	-	-	35.6 [35]	-

Because of the pressure-velocity coupling, the SIMPLE approach was chosen as the solution strategy. The spatial discretization of momentum and energy was set to second-order upwind, whereas the pressure discretization option was set to PRESTO! The transitory formulation was created using the second-order implicit discretization approach. Pressure, density, body forces, momentum, liquid fraction update, and energy have under-relaxation factors of 0.3, 1, 1, 0.7, 0.9, and 1. The convergence conditions for the energy equation are set to 10^{-6} , whereas the convergence

criteria for the continuity equations, velocity, and pressure are set to 10^{-3} . The time step size for the computation was set to 1s.

3. Results

3.1 Validation

The simulation data are validated by comparing them to numerical data from Sellami *et al.*, [29] using RT25, 1000 W/m^2 solar irradiation, with 20°C (293.15K) for the surrounding temperature. The PCM model was developed using layers of 4mm thick aluminium PV. The PCM is 312mm in length plus 20mm wide. Yet, the dimension of the version included in this study is slightly different, at 132mm. In a vertical design, the system's inclination angle remains at 90° . The overall heat loss coefficient was determined to be $5 \text{ W/m}^2\text{K}$ when only the system's backside was analyzed. The other external walls of the system were considered to be adiabatic. The output is given in a transient mode. To confirm the present work's approach, the equations are numerically solved using similar parameters as Sellami *et al.*, [29], with minor modifications according to the constraints. Figure 2 compares temperature profiles at the front PV-PCM system between the current study and Sellami *et al.*, [29].

Despite some modifications done due to the constraints, the mean temperature difference between the simulations is approximately 9.73%, which is well within the acceptable range for validating the current work's model. As a result, this modelling is regarded reliable and sufficient for modelling the thermal regulation of a PV-PCM system with a uniform radiative flux at room temperature.

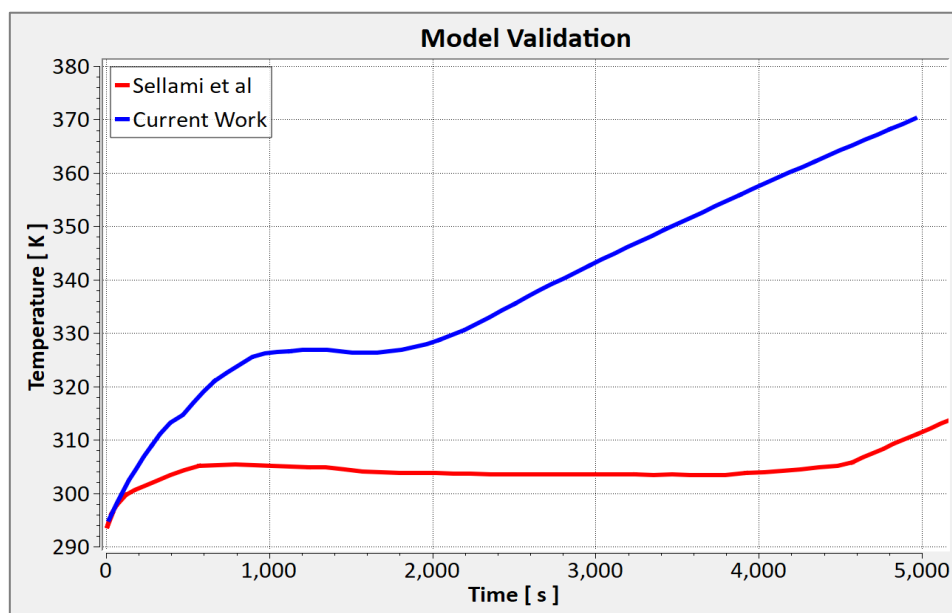


Fig. 2. Model validation via comparison with Sellami *et al.*, [29] and current work

3.2 Temperature Distribution

3.2.1 Effect of PV-PCM tilt angles

Figure 3 compares the effect of varied tilt angles on the heating rate of the PV surface to PV without PCM. Tilting angles range from 0° , 30° , 60° to 90° . The average value of temperature reduction, when compared to the PV system without PCM, increases from 0° (horizontal), 30° , 60° to 90° (vertical) which is 211.4°C , 237.1°C , 239.7°C , and 240.1°C , respectively. PV has the greatest

temperature reduction of 90°C with a drop of 240.1°C and a temperature reduction percentage of 75.7% on average. The maximum average temperature reduction is recorded at t=5000s which is also the maximum reading of the PV-PCM system’s simulation.

Table 3

Thermal variations on the PV surface with different tilt angles, with and without PCM

PV system	Average PV surface temperature (°C)	Maximum average temperature reduction (°C)	Average temperature reduction (°C)	Percentage reduction (%)	
Without PCM	317.0	-	0.0	0.0	
With PCM	0°	105.7	94.3	211.4	66.7
	30°	79.9	103.0	237.1	74.8
	60°	77.4	108.2	239.7	75.6
	90°	76.9	109.4	240.1	75.7

According to the distribution, the 90° tilt angle can reduce the PV surface temperature the most. This may be owing to the vertically mounted PV-PCM increasing the melting rate of the PCM and shortening the time required to reach the melting point of the PCM

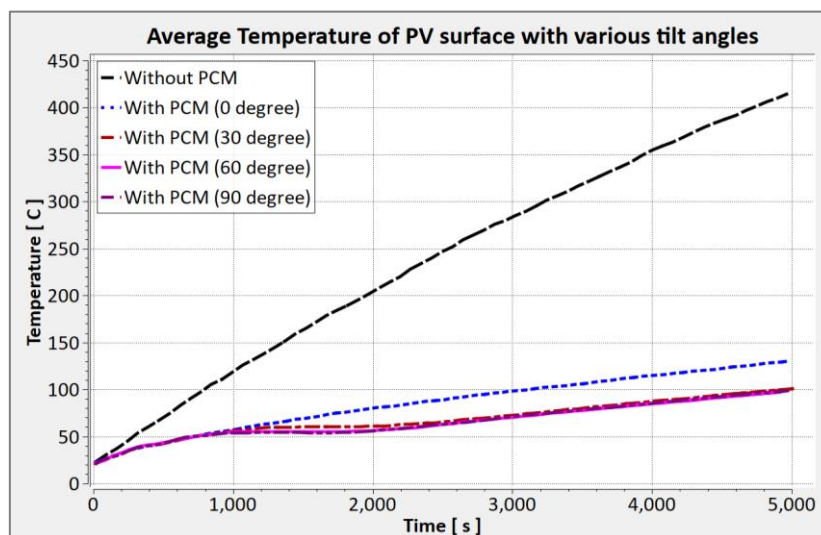


Fig. 3. Temperature distribution of PV surface with various tilt angles

. This impact is readily seen in Figure 4, which displays the temperature contour of the PV-PCM. Conduction occurs as the type of heat transfer between the layers. At t = 1000s, the heat starts to flow onto the PCM layer, reflected by a rise in temperature in that region. Nonetheless, the PCM layer is still not transmitting heat to the back of the system, so the temperature at the back of the system remains at room temperature. At t=1500s to t=2000s, the temperature of the PV surface begins to rise and the heat has already begun to absorb by the PCM. As illustrated in Figure 4, the region of the heat contour across the PCM of the vertical system spreads more than others, contributing to more heat storage from the PV surface than others, indicating that the process of PCM melting is faster than others. At t=3000s, the PCM of the 30°, 60°, and 90° systems are fully liquid, whereas the horizontally aligned system has not yet melted. The melting process of the PCM appears to be accelerated as the tilt angle approaches vertical, which is caused by natural convection flows within the PCM. As natural convection heat transfer within the PCM works better when vertically orientated, the melting rate of the PCM increases [15].

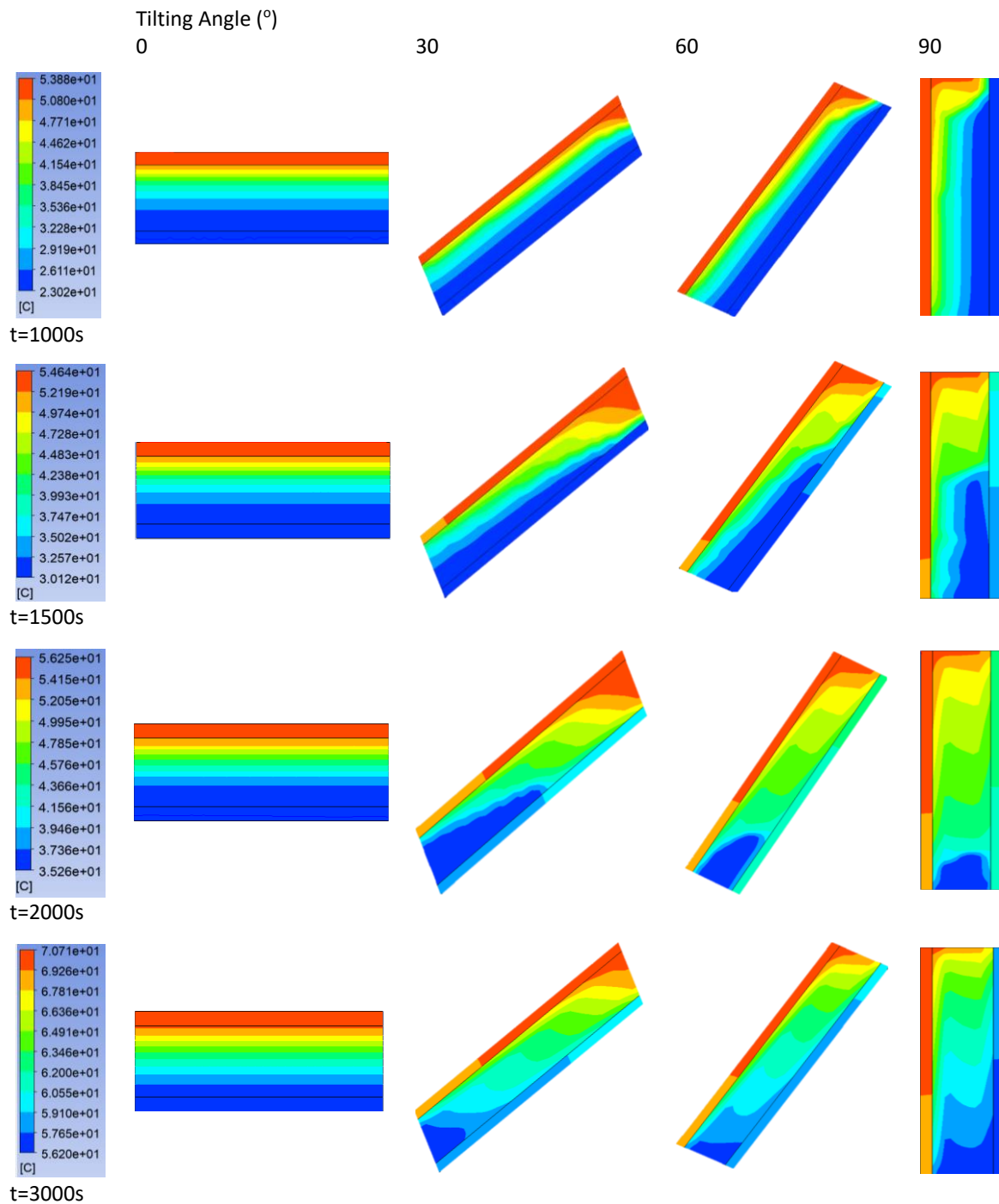


Fig. 4. Temperature contour of PV-PCM with various tilt angles

3.2.2 Effect of PCM thickness

Figure 5 depicts the temperature distribution of a PV surface with different PCM thicknesses placed. The thickness ranges from 20mm to 100mm, with increments of 20mm. PV-PCM with a thickness of 20mm demonstrates the earliest temperature fluctuation of all. The time required for the PCM with a thickness of 20mm to enter the phase transition is only 269s (11.6 minutes), whereas the time required for the PCM with a thickness of 40mm is 1879s (31.32 minutes). Furthermore, PV-PCM with a thickness of 60mm takes 3243s (54.05 minutes) to maintain a constant temperature. The

longest period for the PV to retain the same temperature is 80mm and 100mm, both of which are 4000s (66.67 minutes).

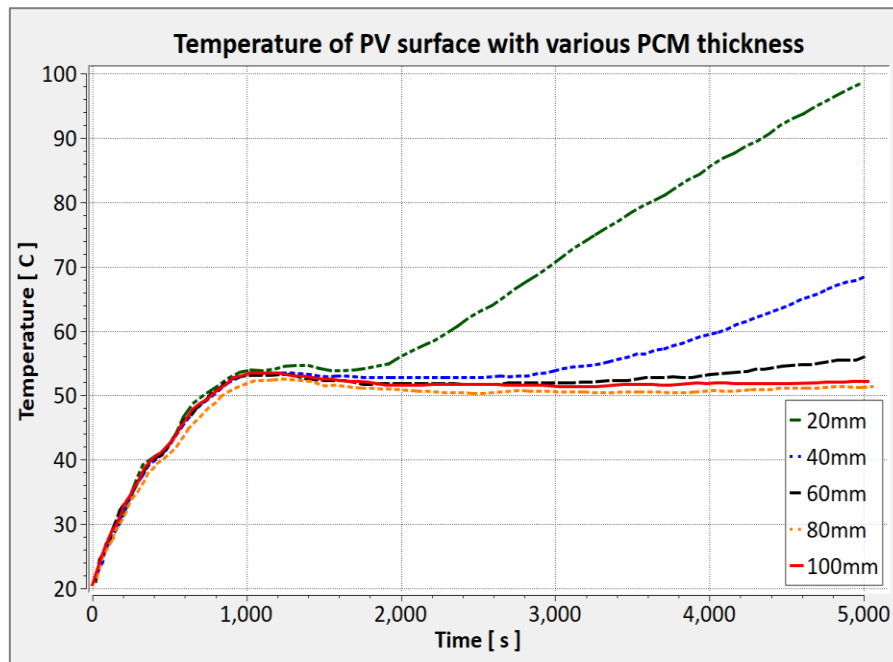


Fig. 5. Temperature distribution of PV surface that affected by various PCM thickness

The figure perfectly indicates that as the PCM thickness increases, the time required for the PV to maintain its temperature between 51°C and 53°C increases. This effect is more visible in Figure 6, which represents the temperature contour of PV-PCM throughout the melting process of the PCM at a vertical position (0°). The vertical position is chosen because the PCM melting process works best in this position, as discussed in the previous section. The PCM goes through phase transitions between temperature ranges, which explains why the temperature is constant for a while. At t=2000s, the melting process for the thinnest (20mm) PCM was nearly complete, but not for other thicknesses, particularly 80mm and 100mm, where a considerable amount of area was still not absorbing heat. As a result, the PCM plays an important function in delivering a greater heat capacity by manipulating its thickness when put in the PV system. However, because the thickness has already reached its capacity, even if the thickness is raised, the time required to maintain the temperature will be equivalent to the optimal thickness, which in this case is 80mm. The findings are also consistent with the conclusion reached by A. Ahmad *et al.*, [18]. They said that PCMs with lower melting temperatures require more PCM even when there is no substantial variation in latent heat.

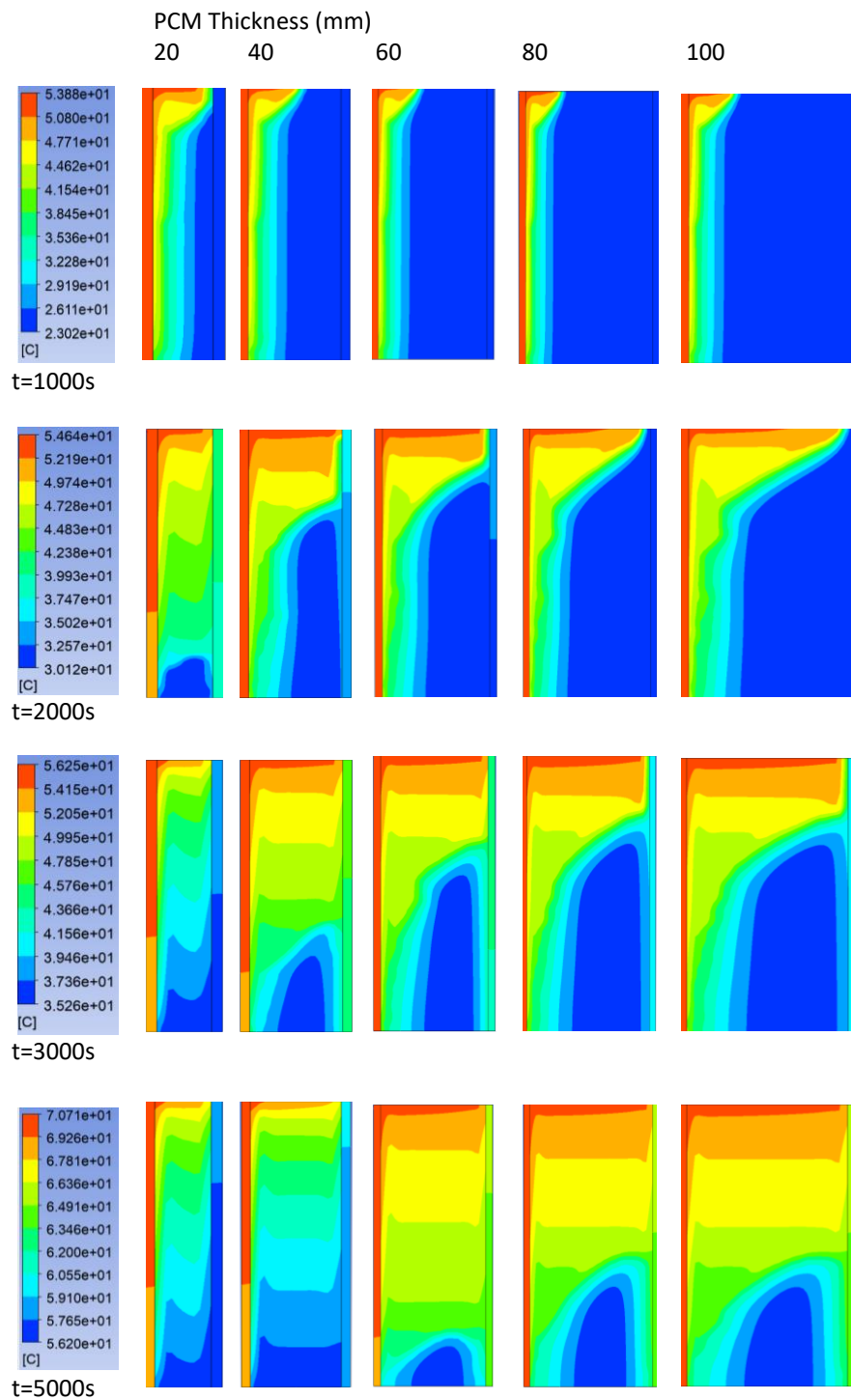


Fig. 6. Temperature contour of PV-PCM that is affected by various PCM thicknesses

3.2.3 Effect of PCM encapsulation material

Figure 7 depicts the temperature distribution of the PV surface with different PCM encapsulating materials (stainless steel, aluminium, and copper). The difference may be seen in the time it takes for the PV surface to reach the melting temperature of the PCM. Aluminium is the first to reach the melting point and enter the phase transition. Since aluminium has the highest specific heat capacity, it can absorb a large amount of heat energy without having a significant temperature increase. This

demonstrates aluminium absorbs heat more than stainless steel and copper, despite having the lowest thermal conductivity of the three.

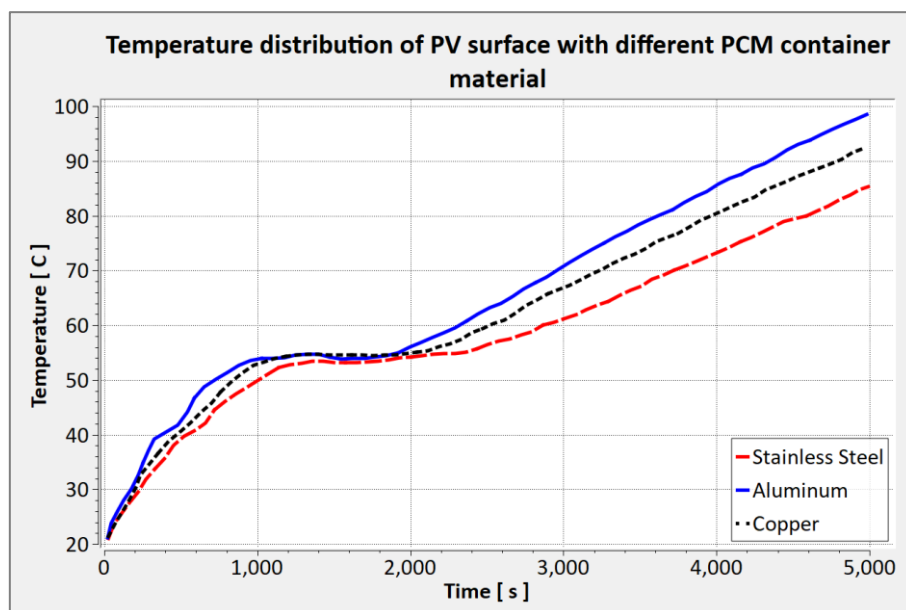


Fig. 7. Temperature distribution on PV surface that is affected by different encapsulation materials, stainless steel, aluminium, and copper

4. Conclusions

In this study, it can be concluded that by manipulating the parametric components of the PV-PCM system, the thermal regulation of the system can be optimized. PCM reaches melting point faster as it tilts from horizontal (0°) to vertical (90°). A vertically oriented PV-PCM system completes the melting process better due to the natural convection heat flows that occur within the PCM being better than the others. The ideal thickness for CPO is 80mm, which can store heat for 4000s (66.67mins) since a larger heat capacity can be absorbed by the PCM with a thicker or larger amount of PCM placed into the system. Despite having the lowest thermal conductivity of the three, aluminium performs better as a PCM encapsulation because it absorbs more heat than stainless steel and copper, allowing the PCM to reach its melting point faster. In systems, CPO has a significant thermoregulation capacity, particularly in Malaysian weather (27°C). More experimental work can be done to validate the findings. Longer times can be explored for the PCM thickness to further analyze the entire time required to fully finish the melting process.

Acknowledgement

The author would like to thank Zamalah Scholarship by Universiti Teknikal Malaysia Melaka and the Applied Solar Energy Laboratory of the Faculty of Mechanical Engineering for their support.

References

- [1] Rosli, Mohd Afzanizam Mohd, Danial Shafiq Mohd Zaki, Fatiha Abdul Rahman, Suhaila Sepeai, Nurfaizey Abdul Hamid, and Muhammad Zaid Nawam. "F-chart method for design domestic hot water heating system in Ayer Keroh Melaka." *Journal of Advanced Research in Fluid Mechanics and Thermal Sciences* 56, no. 1 (2019): 59-67.
- [2] Sachit, F. A., M. A. M. Rosli, N. Tamaldin, S. Misha, and A. L. Abdullah. "Nanofluids used in photovoltaic thermal (pv/t) systems." *International Journal of Engineering & Technology* 7, no. 3.20 (2018): 599-611.
- [3] Elavarasan, Rajvikram Madurai, Vijay Mudgal, Leponraj Selvamanohar, Kai Wang, Gan Huang, G. M. Shafullah, Christos N. Markides, K. S. Reddy, and Mithulananthan Nadarajah. "Pathways toward high-efficiency solar

- photovoltaic thermal management for electrical, thermal and combined generation applications: A critical review." *Energy Conversion and Management* 255 (2022): 115278. <https://doi.org/10.1016/j.enconman.2022.115278>
- [4] Velmurugan, Karthikeyan, Sunilkumar Kumarasamy, Tanakorn Wongwuttanasatian, and Varinrumpai Seithtanabutara. "Review of PCM types and suggestions for an applicable cascaded PCM for passive PV module cooling under tropical climate conditions." *Journal of Cleaner Production* 293 (2021): 126065. <https://doi.org/10.1016/j.jclepro.2021.126065>
- [5] Maleki, Akbar, Arman Haghghi, Mamdouh El Haj Assad, Ibrahim Mahariq, and Mohammad Alhuyi Nazari. "A review on the approaches employed for cooling PV cells." *Solar Energy* 209 (2020): 170-185. <https://doi.org/10.1016/j.solener.2020.08.083>
- [6] Jouhara, Hussam, Alina Żabnieńska-Góra, Navid Khordehgah, Darem Ahmad, and Tom Lipinski. "Latent thermal energy storage technologies and applications: A review." *International Journal of Thermofluids* 5 (2020): 100039. <https://doi.org/10.1016/j.ijft.2020.100039>
- [7] Gharzi, Mostafa, Akbar Arabhosseini, Zakieh Gholami, and Mohammad Hashem Rahmati. "Progressive cooling technologies of photovoltaic and concentrated photovoltaic modules: A review of fundamentals, thermal aspects, nanotechnology utilization and enhancing performance." *Solar Energy* 211 (2020): 117-146. <https://doi.org/10.1016/j.solener.2020.09.048>
- [8] Aridi, Rima, and Alissar Yehya. "Review on the sustainability of phase-change materials used in buildings." *Energy Conversion and Management: X* (2022): 100237. <https://doi.org/10.1016/j.ecmx.2022.100237>
- [9] Tofani, Kassianne, and Saeed Tiari. "Nano-Enhanced phase change materials in latent heat thermal energy storage systems: A review." *Energies* 14, no. 13 (2021): 3821. <https://doi.org/10.3390/en14133821>
- [10] Sitepu, Muhammad Haikal, Abdul Rahim Matondang, and Meilita Tryana Sembiring. "Sustainability assessment in crude palm oil production: A review." In *IOP Conference Series: Materials Science and Engineering*, vol. 725, no. 1, p. 012074. IOP Publishing, 2020. <https://doi.org/10.1088/1757-899X/725/1/012074>
- [11] Sarikarin, Tachakun, Amnart Suksri, and Tanakorn Wongwuttanasatian. "Temperature compensation of photovoltaic cell using phase change materials." *Int. J. Eng. Technol.* 7, no. 3.7 (2018): 179. <https://doi.org/10.14419/ijet.v7i3.7.16345>
- [12] Zhao, Jiaxin, Zhenpeng Li, and Tao Ma. "Performance analysis of a photovoltaic panel integrated with phase change material." *Energy Procedia* 158 (2019): 1093-1098. <https://doi.org/10.1016/j.egypro.2019.01.264>
- [13] Khanna, Sourav, K. S. Reddy, and Tapas K. Mallick. "Performance analysis of tilted photovoltaic system integrated with phase change material under varying operating conditions." *Energy* 133 (2017): 887-899. <https://doi.org/10.1016/j.energy.2017.05.150>
- [14] Abdulmunem, Abdulmunem R., Pakharuddin Mohd Samin, Hasimah Abdul Rahman, Hashim A. Hussien, Izhari Izmi Mazali, and Habibah Ghazali. "Experimental and numerical investigations on the effects of different tilt angles on the phase change material melting process in a rectangular container." *Journal of Energy Storage* 32 (2020): 101914. <https://doi.org/10.1016/j.est.2020.101914>
- [15] Abdulmunem, Abdulmunem R., Pakharuddin Mohd Samin, Hasimah Abdul Rahman, Hashim A. Hussien, Izhari Izmi Mazali, and Habibah Ghazali. "Numerical and experimental analysis of the tilt angle's effects on the characteristics of the melting process of PCM-based as PV cell's backside heat sink." *Renewable Energy* 173 (2021): 520-530. <https://doi.org/10.1016/j.renene.2021.04.014>
- [16] Waqas, Adeel, Jie Ji, Ali Bahadar, Lijie Xu, Zeshan, and Mawufemo Modjinou. "Thermal management of conventional photovoltaic module using phase change materials—An experimental investigation." *Energy Exploration & Exploitation* 37, no. 5 (2019): 1516-1540. <https://doi.org/10.1177/0144598718795697>
- [17] Allah, Malik Al-Abed, and Mahdy Migdady. "Using Design of Experiments Approach to analysis Factors Effecting on the PV Cells." (2020).
- [18] Ahmad, Abdalqader, Helena Navarro, Saikat Ghosh, Yulong Ding, and Jatindra Nath Roy. "Evaluation of new pcm/pv configurations for electrical energy efficiency improvement through thermal management of pv systems." *Energies* 14, no. 14 (2021): 4130. <https://doi.org/10.3390/en14144130>
- [19] Indartono, Y. S., S. D. Prakoso, A. Suwono, I. N. Zaini, and B. Fernaldi. "Simulation and experimental study on effect of phase change material thickness to reduce temperature of photovoltaic panel." In *IOP conference series: materials science and engineering*, vol. 88, no. 1, p. 012049. IOP Publishing, 2015. <https://doi.org/10.1088/1757-899X/88/1/012049>
- [20] Bantová, Sylva, Milan Ostrý, and Karel Struhala. "Interaction between Organic and Inorganic PCMs and Selected Metals." (2019). <https://doi.org/10.20944/preprints201911.0015.v1>
- [21] Abdullah, Amira Lateef, Suhaimi Misha, Noreffendy Tamaldin, Mohd Afzanizam Mohd Rosli, and Fadhil Abdulameer Sachit. "Hybrid photovoltaic thermal PVT solar systems simulation via Simulink/Matlab." *CFD letters* 11, no. 4 (2019): 64-78.

- [22] Sachit, F. A., Noreffendy Tamaldin, M. A. M. Rosli, S. Misha, and A. L. Abdullah. "Current progress on flat-plate water collector design in photovoltaic thermal (PV/T) systems: A Review." *Journal of Advanced Research in Dynamical and Control Systems* 10, no. 4 (2018): 680-89.
- [23] Fatchurrohman, N., and S. T. Chia. "Performance of hybrid nano-micro reinforced mg metal matrix composites brake calliper: simulation approach." In *IOP Conference Series: Materials Science and Engineering*, vol. 257, no. 1, p. 012060. IOP Publishing, 2017. <https://doi.org/10.1088/1757-899X/257/1/012060>
- [24] Kazemian, Arash, Ali Salari, Ali Hakkaki-Fard, and Tao Ma. "Numerical investigation and parametric analysis of a photovoltaic thermal system integrated with phase change material." *Applied energy* 238 (2019): 734-746. <https://doi.org/10.1016/j.apenergy.2019.01.103>
- [25] "MyGOV - Malaysia Information | Climate." (2021) <https://www.malaysia.gov.my/portal/content/144>.
- [26] Vikas, Ankit Yadav, and S. K. Soni. "Simulation of melting process of a phase change material (PCM) using ANSYS (Fluent)." *International Research Journal of Engineering and Technology (IRJET)* 4, no. 5 (2017).
- [27] Luo, Zigeng, Zhaowen Huang, Ning Xie, Xuenong Gao, Tao Xu, Yutang Fang, and Zhengguo Zhang. "Numerical and experimental study on temperature control of solar panels with form-stable paraffin/expanded graphite composite PCM." *Energy Conversion and Management* 149 (2017): 416-423. <https://doi.org/10.1016/j.enconman.2017.07.046>
- [28] Al-Jethelah, Manar SM, Ahmed Al-Sammarraie, Syeda H. Tasnim, Shohel Mahmud, and Animesh Dutta. "Effect of convection heat transfer on thermal energy storage unit." *Open Physics* 16, no. 1 (2018): 861-867. <https://doi.org/10.1515/phys-2018-0108>
- [29] Sellami, Assia, Rabie Elotmani, Khalid Kandoussi, Mohamed Eljouad, Abdelowahed Hajjaji, and M'Hamed Boutaous. "Numerical modelling of phase-change material used for PV panels cooling." *The European Physical Journal Plus* 132 (2017): 1-9. <https://doi.org/10.1140/epjp/i2017-11817-9>
- [30] Yang, Hong-mei, Zhou-meng Pu, Zhi-peng Guo, Ang Zhang, and Shou-mei Xiong. "A study of metal/die interfacial heat transfer behavior of vacuum die cast pure copper." *China Foundry* 17 (2020): 206-211. <https://doi.org/10.1007/s41230-020-9157-8>
- [31] Kant, Karunesh, Amritanshu Shukla, Atul Sharma, and Pascal Henry Biwole. "Heat transfer studies of photovoltaic panel coupled with phase change material." *Solar Energy* 140 (2016): 151-161. <https://doi.org/10.1016/j.solener.2016.11.006>
- [32] Gomna, Aboubakar, Kokouvi Edem N'tsoukpoe, Nolwenn Le Pierrès, and Yézouma Coulibaly. "Review of vegetable oils behaviour at high temperature for solar plants: Stability, properties and current applications." *Solar Energy Materials and Solar Cells* 200 (2019): 109956. <https://doi.org/10.1016/j.solmat.2019.109956>
- [33] Charde, Nachimani. "Microstructure and fatigue properties of dissimilar spot welds joints of AISI 304 and AISI 1008." *International Journal of Automotive and Mechanical Engineering* 7 (2013): 882-899. <https://doi.org/10.15282/ijame.7.2012.7.0072>
- [34] Rahardja, Istianto Budhi, Sukarman Sukarman, and Anwar Ilmar Ramadhan. "Analisis Kalori Biodiesel Crude Palm Oil (CPO) dengan Katalis Abu Tandan Kosong Kelapa Sawit (ATKKS)." *Prosiding Semnastek* (2019).
- [35] Suwono, Aryadi, Moh Irsyad, Yuli Setyo Indartono, and Ari Darmawan Pasek. "EXPERIMENTAL STUDY ON FLOW AND THERMAL CHARACTERS OF CALCIUM CHLORIDE HYDRATE SLURRY." *ASEAN Engineering Journal* 5, no. 2 (2015): 9-16.